Supplemental Materials

Medical Physics Manuscript Title: Temperature and Concentration Dependence of Water Diffusion in Polyvinylpyrrolidone Solutions

By Ghoncheh Amouzandeh, Thomas L. Chenevert, Scott D. Swanson, Brian D. Ross, and Dariya I. Malyarenko

Department of Radiology, University of Michigan, Ann Arbor, MI, USA

Corresponding Author: tlchenev@med.umich.edu

Diffusion gradient calibration: To mitigate diffusion gradient bias error of measured ADC values, we performed gradient calibration for each physical gradient channel (X, Y, Z) used to encode diffusion. For this, the PVP phantom was opened and pre-cooled in an ice-water bath >1hr (Chenevert *et al* JMRI 2011), then filled with an ice-water slurry and sealed such that the central tube (pure water) was equilibrated to 0°C where the diffusion coefficient is known be D_{true} = 1.099μm^2/ms (Holz *et al* PCCP 2000). As with ambient temperature acquisitions, the ice-water filled PVP phantom was scanned in the head coil at magnet isocenter with PVP tube axes aligned along the Z-axis of the 3T scanner. After thermal equilibrium with the surrounding ice-water slurry, 4 dynamics, 2-average, 3-orthogonal (X, Y and Z channel) directional DWI scans were acquired for 7 axial slices centered at magnet isocenter. Calibration of each gradient channel (j) was implemented over an array of b-values: b_{nom} = 0:500:2000 s/mm^2 (Sup. Fig. S1). Matlab scripts were used to estimate a correction factor for each b-value and diffusion direction using the true diffusion coefficient of water = 1.099μm^2/ms at 0°C. Measured signal at nominal b-value, for the *j-th* gradient channel was modeled as:

$$S_{bnom^j} = S_o e^{-btrue^j \cdot D_{true}}, \quad (1)$$

where $btrue^j$ is the actual b-value modeled as a multiplicative function, f_{bv^j}, to the nominal b-value:

$$btrue^j = \frac{1}{D_{true}} \cdot ln\left(\frac{S_o}{S_{bnom^j}}\right) = f_{bv^j} \cdot bnom. \quad (2)$$

Inspection of measured $ln(S_o/S_{bnomj})$ normalized by $D_{true} \cdot bnom$ (Sup. Fig. S1) indicates f_{bvj} were not constant with respect to nominal b-value. Assuming true DWI gradient amplitude, *G*, has an offset error relative to nominal gradient amplitude, and that b-value scales as G^2, the functional form of f_{bvj} was approximated as:

$$f_{bv^j} \approx 1 + p_1 + \frac{p_2}{\sqrt{bnom}}. \quad (3)$$

Volume of interest (VOI) mean DWI signals from the central vial of the ice-water calibration scans were used to derive fit coefficients p_1 and p_2 for each DWI gradient axis thereby providing estimates for the array of $btrue^j$ for each gradient channel. These were subsequently used to estimate water diffusion in PVP at room temperature via linear fit of measured $ln(So/S_{bnomj})$ vs $btrue^j$ performed on a pixel-by-pixel basis for the b-range selected for each PVP sample. Finally, three orthogonal direction ADC maps were averaged to yield each PVP trace ADC value at room temperatures.

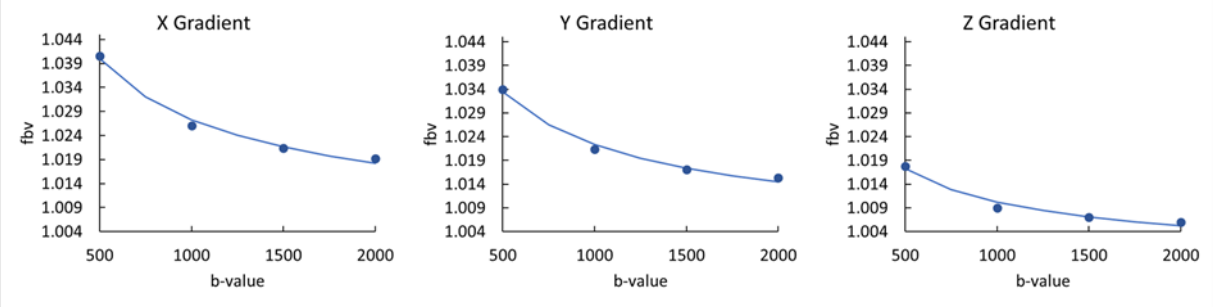

Supplement Figure S1: Gradient b-value calibration function, fbv, determined via ice-water diffusion measurements is illustrated for three gradient channels (left-to-right). fbv is sampled by ratio of measured to nominal ice-water ADC (symbols) as a function of nominal b-value (horizontal axis) and fit to a two-parameter model (lines) described in Sup. Eq(3). Each gradient channel is calibrated independently.

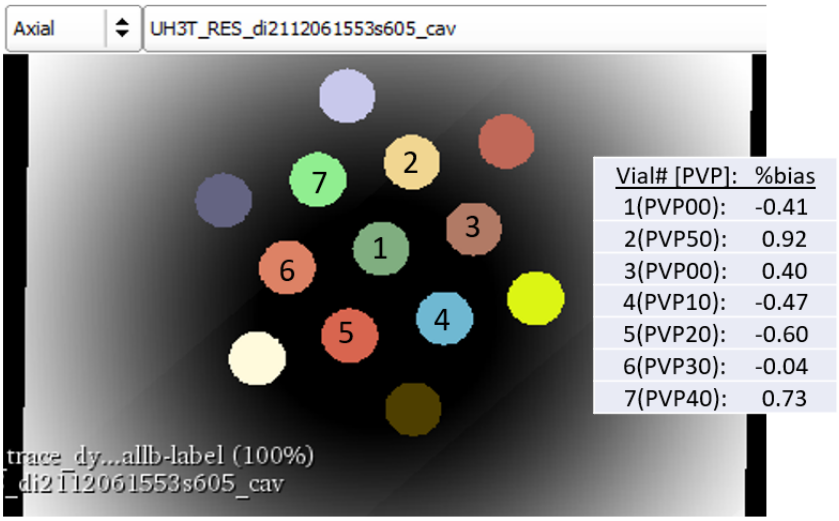

Supplement Figure S2: Spatial bias map of system gradient nonlinearity (GNL) is shown in gray scale with the polyvinyl-pyrrolidone (PVP) phantom regions of interests (ROIs) marked by colored circles that were used for ADC measurements. The table insert summarizes predicted mean ROI bias in b-value due to GNL ($b=b_{nom}/(1+\%bias/100)$), which was corrected for in ADC calculations.

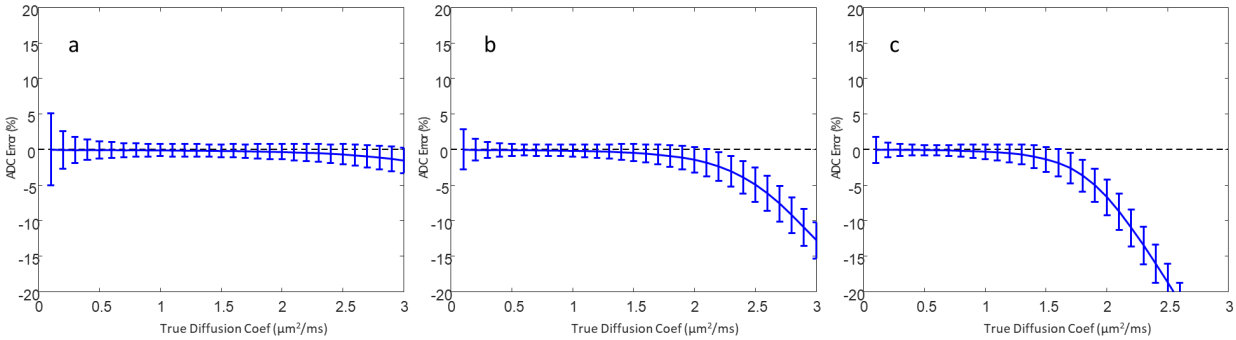

Supplement Figure S3: Sample simulation plots of random (error bars) and noise-floor bias (deviation from dashed line) depending on true diffusion coefficient and maximum b-value used for the fitting. Predicted errors were simulated for observed study conditions of SNR=60 and 10 averages. Plots (a) through (c) correspond to employing bmax of 1000, 1500 and 2000 s/mm^2 respectively.

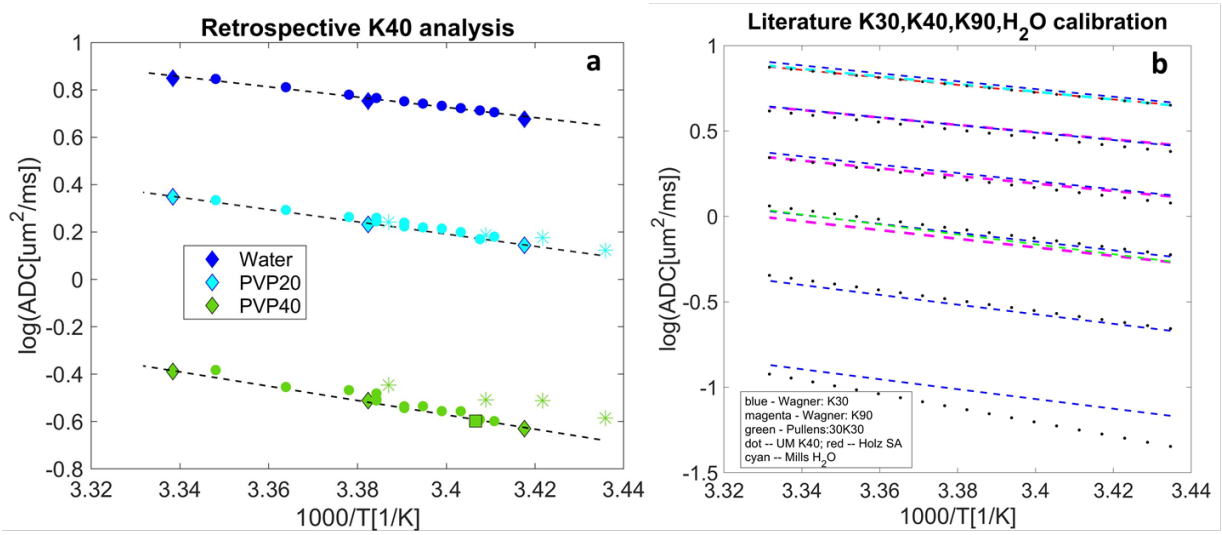

Supplement Figure S4: (a) Log ADC values of water and K40 PVP 20% and 40% measured in this study (diamonds) are plotted with published data from the multi-site reference in circles (Malyarenko et al 2019), asterisks (Keenan 2016, PVP 40% and PVP 20% linearly interpolated from available 18% and 25% PVP data) and a square (Pullens, PVP 40%) with the Arrhenius calibration from the current study (dashed). (b) Summary of literature calibration data for water and diverse molecular weight PVP: Wagner 2017 (blue:K30, magenta: K90), Pullens 2017 (green: 30K30), Holz 2000 (red: Speedy-Angell water), Mills 2014 (cyan: water) and this study (K40: black dots).

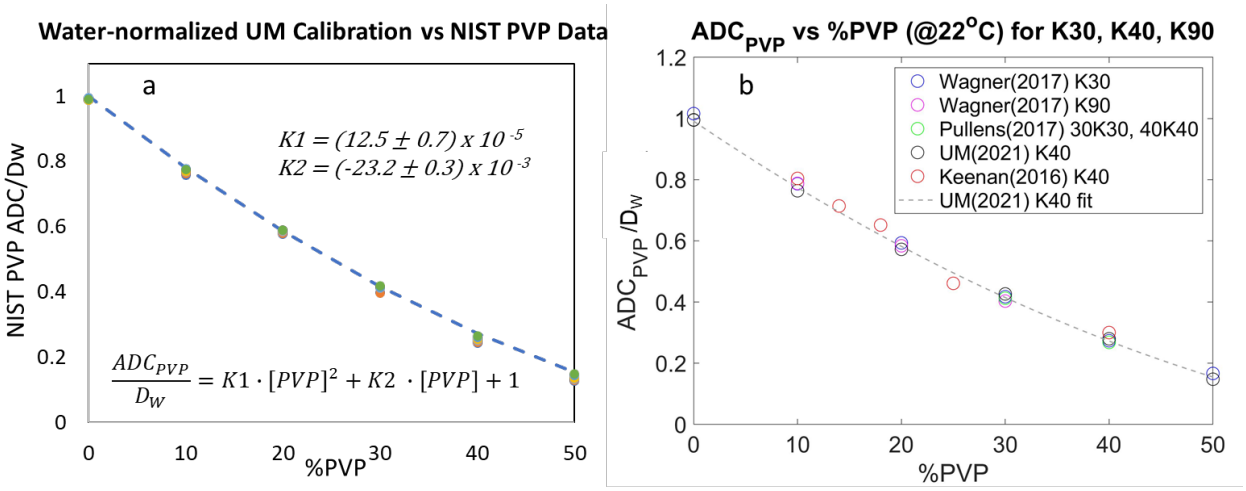

Supplement Figure S5: (a) Concentration dependence for PVP ADC normalized by Speedy-Angell (SA) water diffusion, DW, for temperature-dependent K40 measurements by NIST and (b) multiple prior studies of K30, K40 and K90 at a single 22° C temperature (from literature listed in the legend). Cited values are marked by symbols, and dashed curves in (a) and (b) show the normalized ADC calibration from the current "UM" study.